DEVELOPMENT OF HYDROGEN BEHAVIOR SIMULATION CODE SYSTEM

Atsuhiko Terada[1], Masaaki Matsumoto[2] , Hitoshi Sugiyama[3], Yu Kamiji[1] , Ryutaro Hino[1]

[1] Japan Atomic Energy Agency, 4002 Narita-cho, Oarai-machi, Ibaraki, 311-1393, Japan, terada.atsuhiko@jaea.go.jp
[1] Japan Atomic Energy Agency, 4002 Narita-cho, Oarai-machi, Ibaraki, 311-1393, Japan, kamiji.yu@jaea.go.jp
[1] Japan Atomic Energy Agency, 4002 Narita-cho, Oarai-machi, Ibaraki, 311-1393, Japan, hino.ryutaro@jaea.go.jp
[2] Mitsubishi Research Institute Inc., 10-3 Nagatacho 2-Chome, Chiyoda-ku, Tokyo, 100-8141, Japan, matsumotot@mri.co.jp
[3] Utsunomiya University, 7-1-2 Yotou, Utsunomiya, Tochigi, 321-8585, Japan,sugiyama@cc.utsunomiya-u.ac.jp

ABSTRACT

In the Fukushima Daiichi Nuclear Power Station (NPS) accident, hydrogen generated by oxidation reaction of the cladding and water etc. was leaked into the NPS building, and finally led to occurrence of hydrogen explosion in the building. This resulted in serious damage to the environment. To improve the safety performance of the NPS, especially on the hydrogen safety under severe accident conditions, a simulation code system has been developed to analyze hydrogen behavior including diffusion, combustion, explosion and structural integrity evaluation. This developing system consists of CFD and FEM tools in order to support various hydrogen user groups consisting of students, researchers and engineers. Preliminary analytical results obtained with above mentioned tools, especially with open source codes including buoyancy turbulent model and condensation model, agreed well with the existing test data.

1.0 INTRODUCTION

The accident of the Fukushima Daiichi Nuclear Power Station (NPS) made deepen our awareness on nuclear safety, especially nuclear hydrogen safety. At the severe accident (SA), a large quantity of high temperature steam and chemical substances are released with flammable gas mixed with hydrogen. It is necessary to predict hydrogen distribution in NPS, combustion risk, and its effects [1]. In the world, research organizations and companies have developed and/or improved special analysis codes on hydrogen behaviour such as diffusion, convection, combustion and explosion in order to evaluate hydrogen safety and propose hydrogen safety technologies [2] [3].

2.0 SIMULATION CODE SYSTEM

2.1 SYSTEM DIAGRAM

Based on the phenomenal progress scenario, the system under development is consisted of following three analysis phases: (i) diffusion analysis of leaked flammable gas, (ii) Combustion analyses under deflagration or detonation, (iii) structural analysis against detonation and deflagration. Figure 1 shows the system diagram. In these phases, key models are summarized as follows:

(i) Diffusion analysis of leaked flammable gas

To carry out diffusion analysis of leaked hydrogen gas, it is necessary to consider local density and temperature changes which generate local buoyancy flow. These changes are promoted mainly by steam condensation. Also, the location, quantity and situations of hydrogen release have strong influence to the hydrogen distribution, because hydrogen release leads buoyancy dominated flows

enhancing turbulence by buoyancy effects. Condensation model and buoyancy turbulence model are incorporated in this phase.

(ii) Combustion analyses

Diffusion analysis results are used as initial conditions of this phase, and then combustion analyses including explosive analyses are conducted to obtain a flame speed, a blast pressure under deflagration or detonation along an ignition scenario (ignition time, ignition place etc.). The flame speed and the blast pressure are affected by diffusion spaces and obstacles such as pipings and apparatuses in the space. Flame acceleration model and turbulence combustion model are incorporated in this phase.

(iii) Structural analysis against deflagration or detonation

Blast pressure obtained in combustion analyses is used as an initial condition of this phase. Effect investigation (combustion and explosive effects) is conducted to obtain stress distribution. Then, stress loaded to NPS structures such as steel-reinforced concrete walls and a steel-made container is analyzed to confirm its deformation or destruction of these structures.

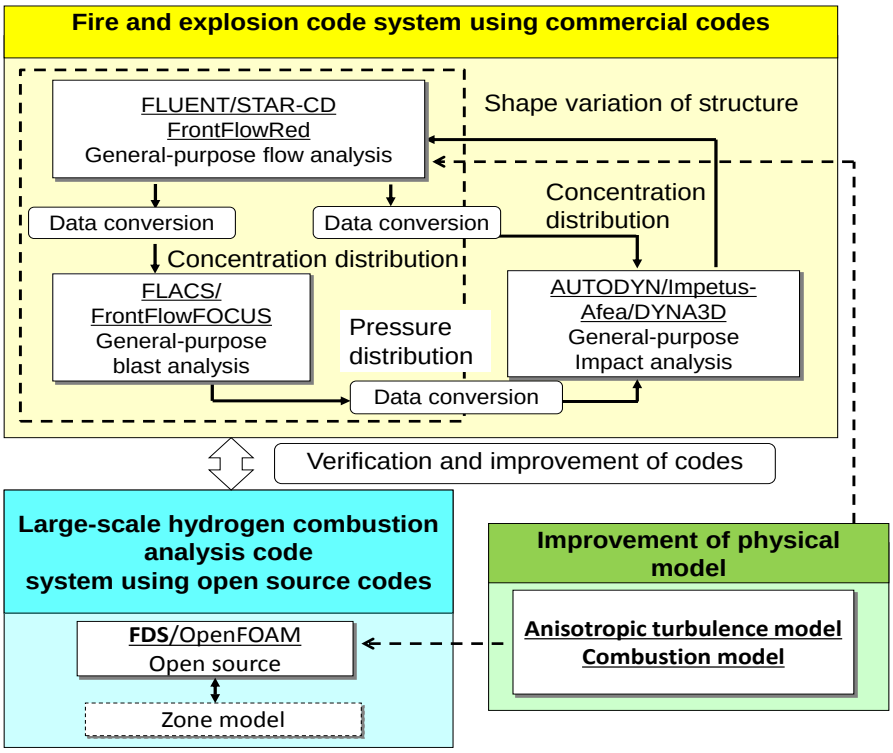

Figure 1. Simulation code system

2.2 OUTLINE OF CODE SYSTEM

The simulation code system consists of general purpose commercial codes available for diffusion, combustion and structural analyses, which named a fire and explosion code system, and open source codes for large-scale hydrogen combustion analysis. Initial condition for the diffusion analysis is provided by a hydrogen generation database which is calculated results of exthermal oxidation of Zircaloy of the fuel cladding and fuel assembly canisters using SA codes (MAAP etc.). Physical

model and mitigation apparatus model (hydrogen recombiner, etc.) for hydrogen safety is being verified and improved using experimental data.

General purpose commercial codes are close cooperation with each other through data conversion interfaces in order to analyse hydrogen diffusion, combustion, effect investigation (explosive effect). Hydrogen concentration in the vessel and building can be simulated with FLUENT [4] and FrontFlowRed [5]. Based on the concentration distribution, users can simulate combustion status such as overpressure on the wall and blast propagation using FLACS [6] and FrontFlowFOCUS [7]. Based on the pressure distribution, users can simulate the stress distribution on the vessel and building wall by AUTODYN [8], DYNA3D [9] and ImpetusAfea [10]. If AUTODYN etc. simulate deformation or damage in the vessel or the wall, shape of analytical model can be changed automatically to the analytical results of deformation or damage, and users simulate flow diffusion analysis by FLUENT etc., again.

FLUENT, FLACS, AUTODYN etc. mentioned above are general-purpose commercial codes based on FEM or FVM methods and have been used for hydrogen behavior analysis. Since these codes are high-cost and has limitation of the improvement of codes, we have been proceeding to develop and apply the open source codes in parallel with the commercial codes.

The open source code system is prepared for various hydrogen users who would like to directly incorporate their own latest knowledge such as physical models and databases into the system. FDS [11] and OpenFOAM [12] can be used for combustion analyses as well as diffusion analyses.

3.0 PRELIMINARY ANALYSIS

3.1 BUOYANCY MODEL IN NPS APPLICATION

Three dimensional buoyancy-opposed wall jet flows were analysed with algebraic Reynolds stress and turbulent heat flux turbulent model including buoyancy turbulent model.

3.1.1 ANISOTROPIC TURBULENCE MODEL

Governing equations are indicated as transport equations of momentum and energy as non-dimensional form as follows;

$$\frac{DU_i}{\partial t} = -\left(\frac{\partial P}{\partial X_i}\right) + \frac{\partial}{\partial X_k}\left(\frac{1}{Re}\frac{\partial U_i}{\partial X_k} - \overline{u_i u_k}\right) + \frac{\beta g T D_{ref}}{U_{ref}{}^2} = -\left(\frac{\partial P}{\partial X_i}\right) + \frac{\partial}{\partial X_k}\left(\frac{1}{Re}\frac{\partial U_i}{\partial X_k} - \overline{u_i u_k}\right) + \frac{Gr}{Re^2}T \quad (1)$$

$$\frac{DT}{\partial t} = \frac{\partial}{\partial X_k}\left(\frac{1}{Re\,Pr}\frac{\partial T}{\partial X_k} - \overline{u_k T'}\right) \quad (2)$$

Transport equation of momentum is also called Reynolds averaged Navier-Stokes equation which is usually abbreviated to RANS. In these equations, Re, Pr and Gr represent Reynolds, Prandtl and Grashof number, respectively. The last term Gr/Re^2 of transport equation of momentum is the buoyancy force effect term, which is called Richardson number Ri. When Richardson number is large, buoyancy forces are important in determining flow patterns.

It is necessary to solve Reynolds stress and turbulent heat flux to obtain velocity and temperature distributions. The anisotropy nature of the turbulence is expressed by the Reynolds stress and turbulent heat flux. In order to deal with anisotropic turbulence precisely, we have adopted the transport equations of Reynolds stress and turbulent heat flux in numerical analysis. The exact formula of these transport equations including buoyancy effect are shown as follows.

$$\frac{D\overline{u_i u_j}}{Dt} = -\left(\overline{u_i u_k}\frac{\partial U_j}{\partial X_k} + \overline{u_j u_k}\frac{\partial U_i}{\partial X_k}\right) + \overline{\frac{p}{\rho}\left(\frac{\partial u_i}{\partial X_j} + \frac{\partial u_j}{\partial X_i}\right)} - \frac{\partial}{\partial X_k}\left\{\overline{u_i u_j u_k} - \nu\frac{\partial \overline{u_i u_j}}{\partial X_k} + \overline{\frac{p}{\rho}\left(\delta_{jk}u_i + \delta_{ik}u_j\right)}\right\} - 2\nu\overline{\frac{\partial u_i}{\partial X_k}\frac{\partial u_j}{\partial X_k}} - \beta\left(g_i\overline{u_j T'} + g_j\overline{u_i T'}\right) \quad (3)$$

$$\frac{D\overline{u_i T'}}{Dt} = -\left(\overline{u_i u_j}\frac{\partial T}{\partial X_j} + \overline{u_j T'}\frac{\partial U_i}{\partial X_j}\right) + \overline{\frac{p}{\rho}\left(\frac{\partial T'}{\partial X_i}\right)} - \frac{\partial}{\partial X_j}\left(\overline{u_i u_j T'} + \overline{\frac{p}{\rho}T'\delta_{ij}}\right) - (\nu + a)\overline{\frac{\partial T'}{\partial X_j}\frac{\partial u_i}{\partial X_j}} - \beta g_i \overline{T'^2} \tag{4}$$

It is impossible to solve directly transport equations of Reynolds stress and turbulent heat flux. Several terms are required to mathematical model. The convection and diffusion terms in the above equations were modeled using Rodi's approximation [13]; i.e.

$$\frac{D\overline{u_i u_j}}{Dt} - Diff_{ij} = \frac{\overline{u_i u_j}}{2k}(P_k - \varepsilon), \qquad \frac{D\overline{u_i T'}}{Dt} - Diff_{iT} = \frac{\overline{u_i T'}}{2k}(P_k - \varepsilon) \tag{5}$$

where $Diff_{ij}$, $Diff_{iT}$ correspond to the third term on the right hand side of Reynolds stress and turbulent heat flux equations, respectively. The production term of turbulent energy is expressed as P_k.Inasmuch as wall functions were used in the present study for the computations, the dissipation rate everywhere in the computed flow was assumed to be locally isotropic; i.e.

$$\varepsilon_{ij} = 2\nu\overline{\frac{\partial u_i}{\partial X_k}\frac{\partial u_j}{\partial X_k}} = \frac{2}{3}\delta_{ij}\varepsilon \tag{6}$$

In the turbulent heat flux equations, the fourth (dissipation) term on the right hand side of the equation was neglected on the basis of assumed high Reynolds number flow.

A particularly problematic task here is the modeling of the pressure-strain correlation term, which is also defined as the redistribution term and is shown as the second term on the right-hand side of the Reynolds stress equation. The pressure-strain term is composed of four parts, which are the interaction of the fluctuating velocities ($\pi_{ij,1}+\pi_{ji,1}$) and the interactions of the mean strain with the fluctuating velocities ($\pi_{ij,2}+\pi_{ji,2}$) and the wall proximity effects ($\pi_{ij,w}+\pi_{ji,w}$) and buoyancy effects ($\pi_{ij,3}+\pi_{ji,3}$). In the present calculation, we have adopted Rotta's linear return to isotropy model for the ($\pi_{ij,1}+\pi_{ji,1}$) term, as shown in Table 1. The interactions of the mean strain with the fluctuating velocities ($\pi_{ij,2}+\pi_{ji,2}$) is modeled basically based on the forth order tensor proposed by Launder et al. [14]. However, the model modified by Sugiyama et al is adopted in the calculations. In terms of the modeling of ($\pi_{ij,2}+\pi_{ji,2}$), the modeling process is described in detail in the report by Sugiyama et al. [15]. The wall effect term ($\pi_{ij,w}+\pi_{ji,w}$) on turbulent stresses and buoyancy effects are modeled as shown in Table 1. In Table 1, f(L/Xw) is a function related to the dimensionless distance from the wall, and cμ and κ represent the empirical constant and the von Karman constant, respectively. The function f(L/Xw) is of unit value near the wall and approaches zero with increasing distance from the wall. The symbol Xw is the normal distance from the wall, and L defines the length scale of turbulence.

When f(L/Xw) is zero, the model yields the correct Reynolds stress components for the nearly homogeneous share flow of Champagne et al. [16] The coefficient values of the pressure-strain correlation term are specified in Table 2.

It is also necessary to express the pressure-temperature gradient term as the mathematical model as well as pressure strain term. The pressure-temperature gradient term is modeled as shown in Table 3.

Table 1. Modeling of the pressure-strain correlation term

$\pi_{ij,1}+\pi_{ji,1}$	$-C_1\frac{\varepsilon}{k}\left(\overline{u_i u_j}-\frac{2}{3}k\delta_{ij}\right)$
$\pi_{ij,2}+\pi_{ji,2}$	$-\frac{C_2+8}{11}(P_{ij}-\frac{2}{3}P_k\delta_{ij})+\varsigma k\left(\frac{\partial U_i}{\partial X_j}+\frac{\partial U_j}{\partial X_i}\right)$ $-\frac{8C_2-2}{11}(D_{ij}-\frac{2}{3}P_k\delta_{ij})$
$\pi_{ij,w}+\pi_{ji,w}$	$C_1=C_1^*+C_1^{'}f\left(\frac{L}{X_w}\right),\quad C_2=C_2^*+C_2^{'}f\left(\frac{L}{X_w}\right)$ $\varsigma_2=\varsigma_2^*+\varsigma_2^{'}f\left(\frac{L}{X_w}\right)$
$\pi_{ij,3}+\pi_{ji,3}$	$-C_3\left(P_{ij,b}-\frac{2}{3}P_b\delta_{ij}\right)$
$P_{ij}=-\overline{u_iu_k}\frac{\partial U_j}{\partial X_k}-\overline{u_ju_k}\frac{\partial U_i}{\partial X_k}, D_{ij}=-\overline{u_iu_k}\frac{\partial U_k}{\partial X_i}-\overline{u_ju_k}\frac{\partial U_k}{\partial X_i}, P_k=-\overline{u_ku_l}\frac{\partial U_k}{\partial X_l}$ $P_{ij,b}=-\beta\left(g_i\overline{u_jT'}+g_j\overline{u_iT'}\right),\quad P_b=-\beta g_i\overline{u_iT'},\quad f\left(\frac{L}{x_w}\right)=\frac{C_\mu^{3/4}k^{3/2}}{\kappa\varepsilon X_w}$	

Table 2. Constants of the Pressure-strain correlation term

C_1^*	C_2^*	ς^*	C_1'	C_2'	ς'	C_μ	κ	C_3
1.4	0.44	-0.16	-0.35	0.12	-0.1	0.09	0.42	0.3

As for modeling slow return effects, Lumley [17] modified the model presented by Monin [18] by introducing an anisotropic tensor into the model coefficients, which yielded the expression for $\pi_{iT,1}$. In order to model rapid return effects, the model proposed by Lumley [17] and independently by Launder [19] was adopted in this study. Inasmuch as wall effects on the model coefficients are important, coefficient values are evaluated from the expressions, which take into account wall proximity effects. In this research, buoyant force effect $\pi_{iT,3}$ is neglected because of small value. Pressure-temperature gradient term is modeled as shown in Table 3. The model constants are listed in Table 4.

The transport equations of turbulent energy and dissipation are needed to obtain Reynolds stress and turbulent heat flux. These equations are expressed in the following form:

$$\frac{Dk}{Dt} = \frac{\partial}{\partial X_j}\left\{\left(\nu\delta_{jk} + c_s \frac{k}{\varepsilon}\overline{u_k u_j}\right)\frac{\partial k}{\partial X_k}\right\} - \overline{u_i u_k}\frac{\partial U_i}{\partial X_k} + P_b - \varepsilon \tag{7}$$

$$\frac{D\varepsilon}{Dt} = \frac{\partial}{\partial X_j}\left\{\left(\nu\delta_{jk} + c_\varepsilon \frac{k}{\varepsilon}\overline{u_k u_j}\right)\frac{\partial \varepsilon}{\partial X_k}\right\} - \frac{\varepsilon}{k}\left(c_{1\varepsilon}\overline{u_i u_k}\frac{\partial U_i}{\partial X_k} + c_{2\varepsilon}\varepsilon - c_{3\varepsilon}P_b\right) \tag{8}$$

Model constants c_s, c_ε, $c_{1\varepsilon}$, $c_{2\varepsilon}$ and $c_{3\varepsilon}$ are 0.22, 0.18, 1.44, 1.92 and 1.44, respectively.

Table 3. Modeling of the pressure-temperature gradient term

$\pi_{iT,1}$	$-C_{1T}\frac{\varepsilon}{k}\overline{u_i T'} - C'_{1T}\frac{\varepsilon}{k}\left(\frac{\overline{u_i u_j}}{k} - \frac{2}{3}\delta_{ij}\right)\overline{u_j T'}$
$\pi_{iT,2}$	$C_{2T}\overline{u_m T'}\frac{\partial U_i}{\partial X_m} - C'_{2T}\overline{u_m T'}\frac{\partial U_m}{\partial X_i}$
$\pi_{iT,w}$	$C_{1T} = C^*_{1T}\left\{1 + C_{1T,w}\cdot f\left(\frac{L}{X_w}\right)\right\}$ $C'_{1T} = C'^*_{1T}\left\{1 + C_{1T,w}\cdot f\left(\frac{L}{X_w}\right)\right\}$ $C_{2T} = C^*_{2T}\left\{1 + C_{2Tw}\cdot f\left(\frac{L}{X_w}\right)\right\}$ $C'_{2T} = C'^*_{2T}\left\{1 + C_{2T,w}\cdot f\left(\frac{L}{X_w}\right)\right\}$
$\pi_{iT,3}$	$-C_{3T}\beta g_i\overline{T'^2}$
$\overline{T'^2} = -\frac{1}{C_{4T}}\frac{\varepsilon}{k}\overline{u_k T'}\frac{\partial \overline{T}}{\partial X_k}$	

Table 4. Constants of the pressure-temperature gradient term

C_{1T}^{*}	$C_{1T}^{'*}$	C_{2T}^{*}	$C_{2T}^{'*}$	$C_{1T,w}$	$C_{2T,w}$	C_{3T}	C_{4T}
3.9	-2.5	0.8	0.2	0.25	-0.46	0.0	0.62

3.1.2 NUMERICAL TEST SECTION

Figure 2 shows the numerical test section which is almost the same as the experimental apparatus presented by He et al [20]. The test section which was a vertical passage of rectangular cross section (length 1.2m, width 0.3m and height 2.3m), had transparent walls to enable laser optical measurement of the flow to be made. As shown in Figure 2, a plane jet of warm water issuing downwards from an 18mm gap between a glass plate of thickness 20mm and one wall of the test section encountered a slowly ascending stream of cool water. In other words, warm jet flow runs into open space from right hand side channel of rectangular duct has an aspect ratio of four to one. Since inertial and buoyant forces act in opposite direction to each other, the jet flow direction changes from downward to upward. Spreading and deceleration of the jet flow occurred until it eventually turned upward on joining the counter-current stream. Combined flow was withdrawn from the top of the test section. The aspect ratio of the jet was 67:1 and that of the test section was 4:1. As shown in this figure, long duct is provided in downward direction. Duct length is 100 times of jet width D. Besides, it is noted that uniform background current runs from bottom inlet upwards. The ratio of background velocity to jet velocity is 0.077.

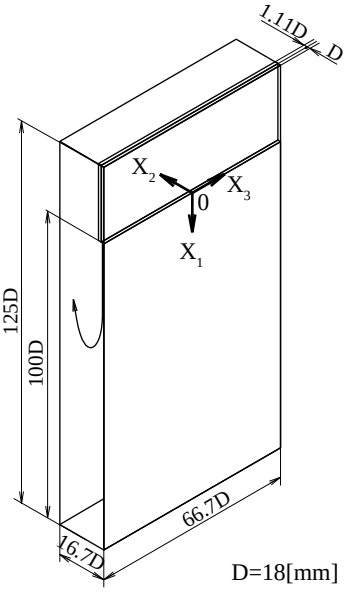

Figure 2. Schematic numerical test section and coordinate system

As for the numerical calculation, several results have been reported until now. These calculated results suggest that this turbulent wall jet with heat transfer is difficult to predict even if flow is isothermal field because anisotropic turbulence and heat flux are produced actively near the wall [21],[22]. Craft et al. [23] have carried out a numerical analysis for the buoyant turbulent wall jet measured by He et al. They have reported that the two-equation turbulent model is unable to predict precisely the flow pattern. These results also suggest that to obtain reasonable predictions one needs to solve transport equations for the Reynolds stress and turbulent heat flux rather than assume an isotropic eddy viscosity.

3.1.3 NUMERICAL ANALYSIS

Figure 3 shows two computational grids which are layout from different point of view. The left hand side of Figure 3 is grid layout from side view of a rectangular duct and the right hand side of that is the sectional grid-layout from top view of a rectangular duct. The inlet length of the rectangular duct is the same as that of the experimental apparatus. The initial values of turbulent energy and dissipation were assumed to be $k = U_b^2 x 10^{-5}$ and $\varepsilon = k^{3/2}/D$,

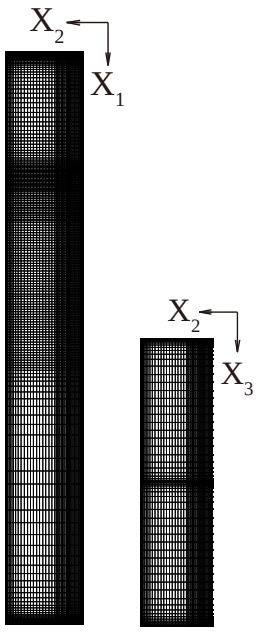

Figure 3. Calculation grid layout in X_1-X_2 and X_2-X_3 planes

respectively. Since the proposed turbulent model can be classified as a high-Reynolds-number turbulent model, the wall function method is adopted as the boundary condition for the turbulent energy and dissipation at the first grid point from the wall. Fine grids are used near the wall because the physical parameters changes rapidly near the wall. The governing equations were discretized by the differencing scheme, and QUICK (a third-order up-wind differencing scheme) was used for the convection term. In this analysis, calculation has been carried out for three kinds of Richardson number (Ri), which are 0, 0.01 and 0.02. These Richardson numbers are obtained by using the jet width and the jet velocity and Reynolds number is also calculated as 4754. The cross section of X_2-X_3 plane has 45x23 computational grid points, and 196 grid points are set along the main flow direction. Therefore, the total number of computational grid points is 202,860.

3.1.4 RESULTS AND DISCUSSION

In this paper. we will introduce the results of Ri=0.02. Figure 4 shows the comparison of mean velocity flow vectors in the case of Ri=0.02. Compared results indicate clearly that turning location of jet flow moves more upward place with increasing Richardson number. The turning location of jet flow from downward to upward is recognized at about $X_1/D=21$ in both results. The flow pattern of circulation predicted by calculation is similar to that of the experiment.

In order to estimate the effect of Richardson number, He et al. introduced a penetration distance of the jet which is defined as the distance from jet exit to the location at which the normalized value of temperature minus background stream temperature falls to about a value of 0.02. Therefore, it is necessary to predict precisely the temperature field to get the penetration distance of the jet correctly.

Figure 5 indicates the comparison of penetration distance of the jet flow. In this figure, the experimental data measured by Goldman and Jaluria [24] are also shown as reference. Definition of penetration distance of the jet is the same in both experiments. Clearly, the reduction of jet penetration with the increase of the Richardson number is stronger than that found by Goldman and Jaluria. In the experiment of Goldman and Jaluria, the top and bottom walls were open which is different between both experiments. As for Ri=0.01, calculated penetration distance is close to Goldman's data rather than He's data. However, the calculated result of Ri=0.02 is in agreement with both experimental results.

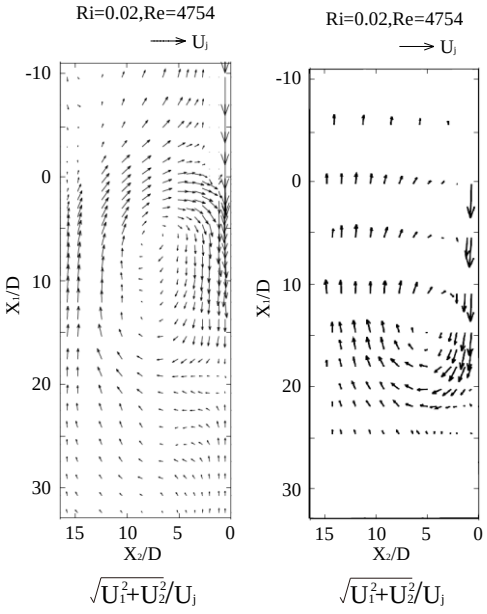

Prediction Experiment by He, et al.

Figure 4. Comparison of mean flow velocity vectors in the case of $Ri = 0.02$

It has been confirmed from the comparison of mean velocity vectors and penetration distance of jet that the presented turbulent model including buoyant force is able to predict the characteristic feature of buoyancy opposed wall jet flow, although the agreement with the experiment is not perfect in all detail.

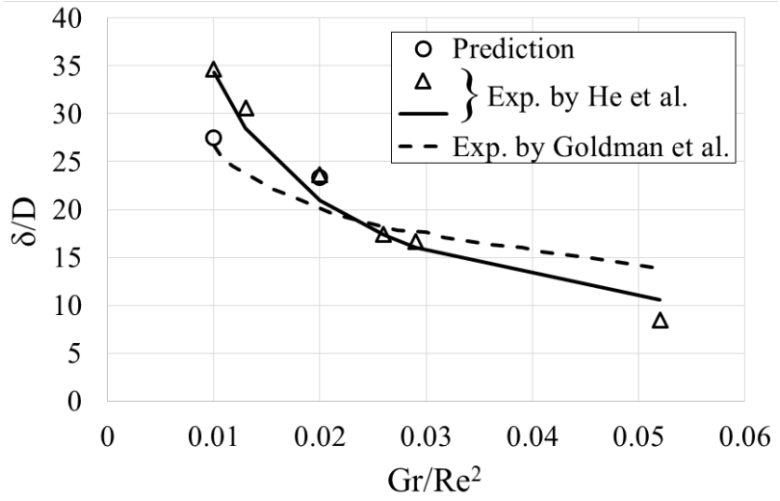

Figure 5. Comparison of penetration distance of jet

3.2 CONDENSATION MODEL ON WALL IN NPS APPLICATION

At the NPS accidents, the containment vessel and the reactor building will be exposed high temperature and high humidity due to the spray cooling or the leak of the cooling water. Under the condition, wall condensation will affect flow behaviour in the vessel and building. In addition to analyses on buoyancy effects mentioned before, wall condensation effects were confirmed with FDS code.

3.2.1 MATHEMATICAL CONDENSATION MODEL

Wall condensation was modelled with following mass transfer equation at wall [25]:

$$\dot{m} = S \times \mathrm{Sh} D/L \rho \ln\left(\frac{P-P_s}{P-P_h}\right) \quad (9)$$

where, D, L, P, P_h, P_s, S, and ρ are diffusion coefficient of gas, diffusion length, total pressure, partial pressure of water vapor, saturation pressure of water vapor to the wall temperature, area at a wall and density of gas, respectively. Transfer of energy due to wall condensation is given by the product of the mass transfer and the latent heat h_{fg}.

$$\dot{h} = \dot{m} \times h_{fg} \quad (10)$$

This model was implemented in FDS.

3.2.1 NUMERICAL ANALYSIS OF TOSQAN ISP-47

The wall condensation model was verified with TOSQAN ISP-47 experimental results [26]. TOSQAN ISP-47 experiment is characterized by four steady-state conditions in a test vessel; three steady-state conditions werw realized under air-steam mixture at two different pressure levels, and one steady-state condition under air-steam-helium mixture. These steady-state conditions were set by interaction between steam injection and wall condensation.

Figure 6 shows the comparison between analytical and experimental results. As seen in the figure, FDS code coupled with the wall condensation model simulated the experimental results very well.

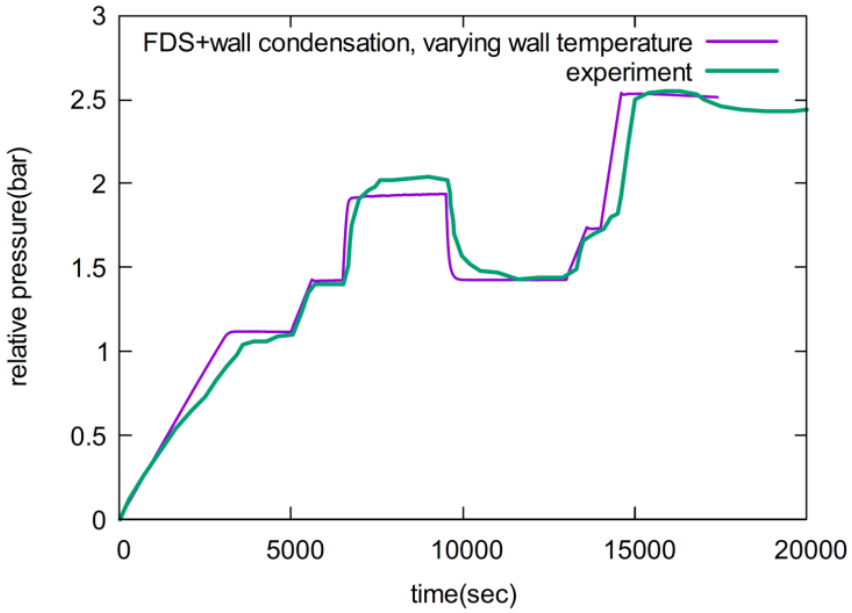

Figure 6. Comparison with experimental result

4.0 CONCLUDING REMARKS

The simulation code system on hydrogen behaviour is being developed to contribute to SA analyses. Preliminary analysis using the system was conducted to validate its performance, especially in the field of buoyancy and condensation phenomena effects using the open source codes. This system will be improved step by step by verifying the codes using the existing database such as the OECD/NEA benchmark program etc. and our own dataset. We will provide the system to engineers, researchers and students in the near future.

ACKNOWLEDEMENTS

The present study was performed in the Advanced Nuclear Hydrogen Safety Research Program funded by Agency for Natural Resources and Energy of Ministry of Economy, Trade and Industry.

REFERENCES

1. TECDOC I., 2011. Mitigation of Hydrogen Hazards in Severe Accidents in Nuclear power Plants , Tech,Rep.IAEA-TECDOC-1661.IAEA
2. OECD/NEA I.,2014.Status Report on Hydrogen management and Related Computer Codes, Tech, Rep. NEA/CSNI/R(2014)8
3. OECD/NEA I., 2008. Assessment of Computational Fluid Dynamics (CFD) for Nuclear Reactor Safety Problems, Tech, Rep. NEA/CSNI/R(2007)13
4. http://ansys.jp/products/fluid/fluent/
5. http://www.nufd.jp/product/nufd_frontflowred.html
6. http://www.gexcon.com/flacs-software
7. http://www.advancesoft.jp/product/index.html
8. http://ansys.jp/products/explicit/autodyn/

9. http://www.oecd-nea.org/tools/abstract/detail/ests0138
10. http://impetus-afea.com/
11. http://code.google.com/p/fds-smv/
12. http://www.openfoam.com/
13. Rodi, W., A new algebraic relation for calculating the Reynolds stresses. ZAMM (56), 1976, T219-T221.
14. Launder, B.E., Reece, G.J. and Rodi, W., Progress in the development of a Reynolds stress turbulent closure. J. Fluid Mech. 22, 1975, pp.537-566.
15. Sugiyama, H. and Hitomi, D., Numerical analysis of developing turbulent flow in a 180° bend tube by an algebraic Reynolds stress model. Int. Journal for Numerical Methods in Fluid. 47, 2005, pp.1431-1449.
16. Champangne, F. H., Harris, V. G. and Corrsin, S., Experimental on nearly homogeneous turbulent shear flow. J. Fluid Mech. 41, 1970, pp. 81-139.
17. Lumley, J. L., Introduction. In Prediction methods for turbulent flows. Lecture Series **76**, 1975, von Karman Inst., Belgium.
18. Monin, A. S., On the symmetry properties of turbulence in the surface layer of air. Atmos. and Oceanic Phys. **1 (1)**, 1965, pp.25-30.
19. Launder, B. E., Heat and mass transport. In Turbulence, Topics in Applied Physics 12. Springer-Verlag, Berlin Heidelberg, Germany, 1976, pp.231-287.
20. He,S., Zu, Z. and Jackson, J.D., An experimental investigation of buoyant-opposed wall jet flow. Int. Journal of Heat and Fluid Flow. 23, 2001, pp.487-496.
21. Launder, B.E. and Rodi, W., The turbulent wall jet – measurements and modelling. Annual Review of Fluid Mechanics. 15, 1983, pp.429-459.
22. Craft, T.J. and Launder, B.E., On the spreading mechanism of the three-dimensional turbulent wall jet. J. Fluid Mech. 435, 2001, pp.305-326.
23. Craft, T.J., Gerasimov, A.V., Iavovides, H., Kider J.W. and Launder, B.E., The negatively buoyant turbulent wall jet: performance of alternative options in RANS modeling. Int. Journal of Heat and Fluid Flow. 25, 2004, pp.809-823.
24. Goldman, D. and Jaluria, Y., Effect of opposing buoyancy on the flow in free and wall jets. J. Fluid Mech. 166,1986, pp.291-301.
25. Herranz LE, Anderson MH, Corradini ML, "Diffusion layer model for steam condensation within the AP600 containment", Nuc. Eng. Des. 183,1998, pp.133-150.
26. OECD/NEA I., 2007. INTERNATIONAL STANDARD PROBLEM ISP-47 ON CONTAINMENT THERMAL HYDRAULICS FINAL REPORT. Tech, Rep.NEA/CSNI/R(2007)10